Dipolar and Quadrupolar Signatures of Topological Band Structures

Louis Bouchard

UCLA

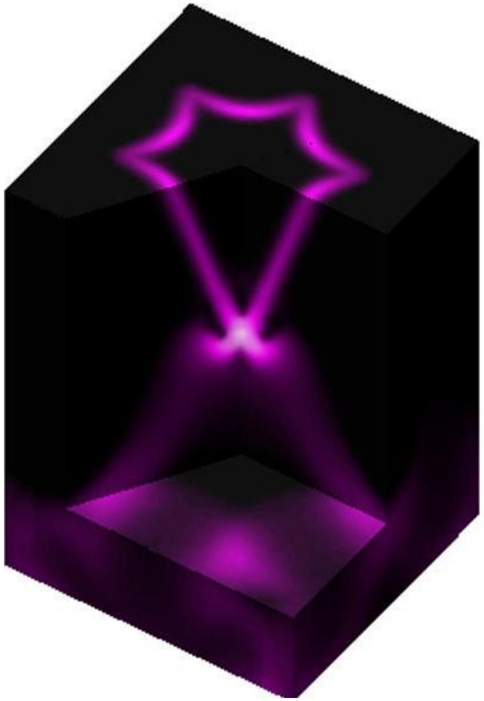

October 21, 2014

topological band structures

and the role of electronic and nuclear spins

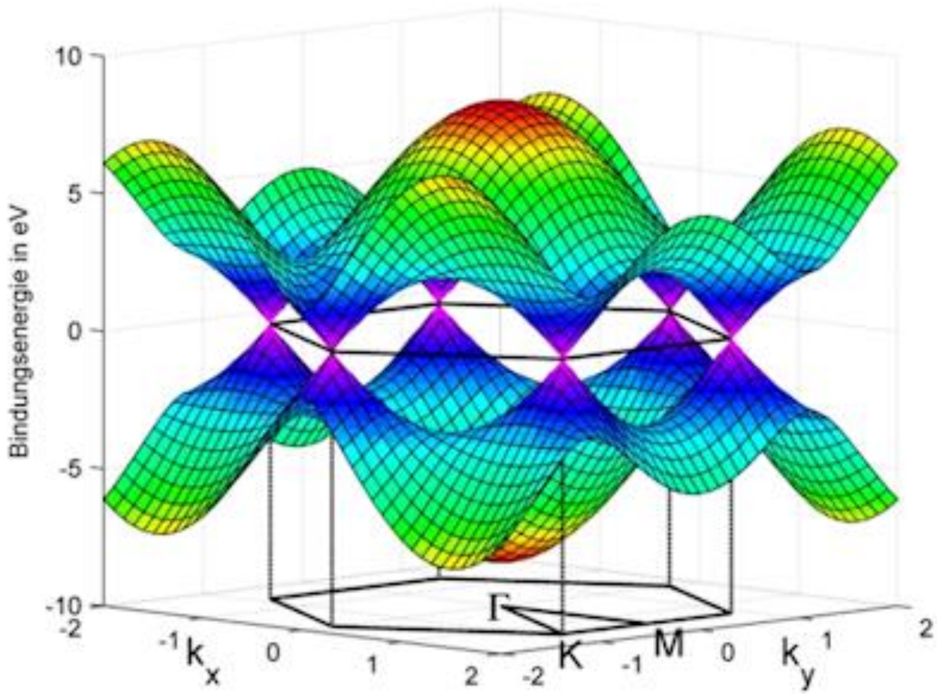

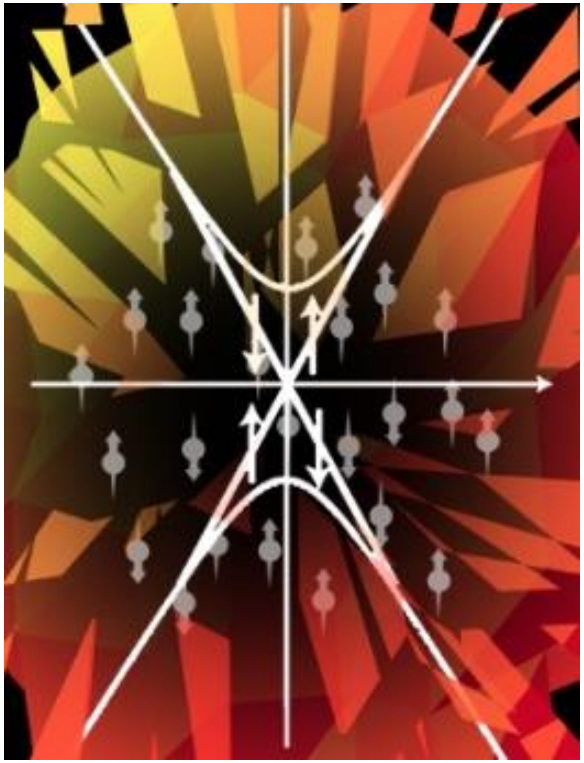

Phys. Rev. Lett. **110**, 026602 (2013); *J. Phys. Chem. C* **117**, 8959 (2013); *J. Phys. Chem. C* **116**, 17300 (2013); *Adv. Func. Mater.* **24**, 1519-28 (2013)

Topological Insulators

Studies of Surface States

Studies of Bulk Properties

Topological Crystalline Insulators

Topological Insulators

new state of matter with **particular topology** of the band structure:

insulating in the bulk due to the existence of a bulk band gap

intrinsic 2D surface state with linear E(k) dispersion at the surface

TI materials are insulators inside and conductors outside, in analogy to quantum Hall state of 2D electron gas systems in magnetic fields.

properties of topological surface

gapless non-spin degenerate Dirac cone

spin of electrons is locked with in-plane $k_{//}$ wave vector,

spin-polarized current flow

protected by time reversal symmetry against scattering and perturbations

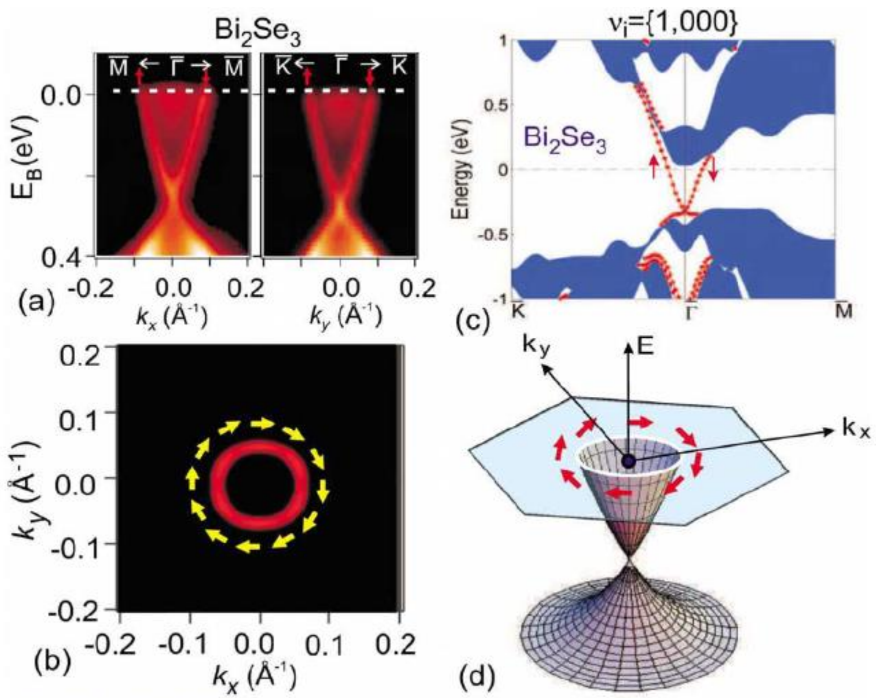

NATURE PHYSICS | VOL 5 | JUNE 2009 |

theoretical prediction

Kane, Mele, Fu (PRL 2005, 2007),

Bernevig et al. (Science 2006)

experimental observation

2D: HgCdTe QWs (König 2007), 3D: $Bi_{1-x}Sb_x$ (Hsieh 2008), Bi_2Se_3 (Xia 2009)

properties of interest in applications

bulk band structure (e.g. band gap), magnetism, defects (vacancies, antisite, dislocations etc.)
surface massless, Dirac-cone-like surface states, surface magnetism, s-o interaction → spin locked to electron momentum k, TRS → no backscattering

want insulating bulk, conductive surface (in fact, non-trivial), and high “contrast” in measurements up to RT.

current techniques

ARPES, STM, transport, optical, TEM, etc. work well but sometimes mix bulk & surface, and require LT.
Capping layer, film thickness, reproducibility

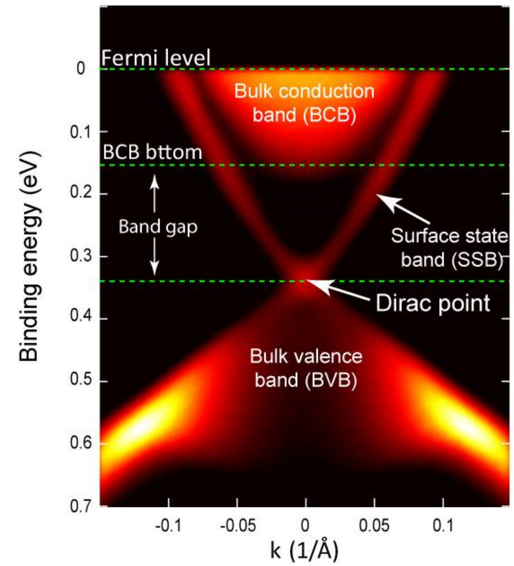

Y Xia, arXiv 2008; Wray et al, *Nat. Phys.* 2010

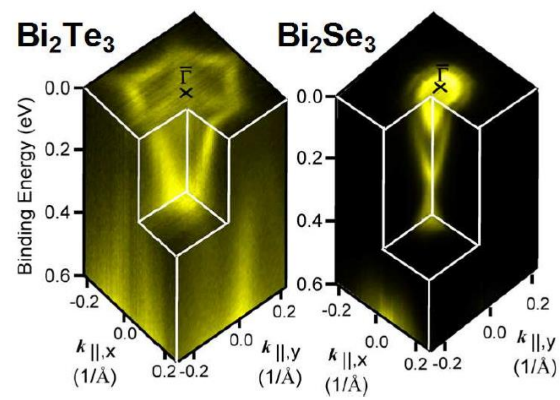

Also ternary alloys (Heuslers): X_2YZ or XYZ

our project aims to probe both *n*- and *p*-type materials, with defects, and up to rt

selectivity to bulk vs surface

non-ideal materials, defects

NMR reports on carrier concentration density of states,
magnetic order, effective mass, etc.

nanoscale resolution

heterostructures, interfaces

Topological Insulators

Studies of Surface States spin-hamiltonian

Studies of Bulk Properties

Topological Crystalline Insulators

nuclear spin-hamiltonian

$$H_{dipole} = -2\mu_B \gamma_n \hbar \mathbf{I}\left[\frac{\mathbf{S}}{r^3} - \frac{3\mathbf{r}(\mathbf{S}\cdot\mathbf{r})}{r^5}\right]$$

$$H_{orbital} = -\gamma_n \hbar \frac{e}{mc}\left[\frac{\mathbf{I}(\mathbf{r}\times\mathbf{p})}{r^3}\right]$$

$$\mathcal{H} = \mathcal{H}_Z + \mathcal{H}_{hf} + \mathcal{H}_Q + \mathcal{H}_d + \mathcal{H}_{orb}$$

$$H_Q = \frac{e^2 qQ}{4I(2I-1)}\left[3I_z^{\,2} - \vec{I}^{\,2} + \frac{1}{2}\eta\left(I_+^{\,2} + I_-^{\,2}\right)\right]$$

$$\mathcal{H}_Z = -\gamma\hbar H_0 \sum_i I_z^{(i)}$$

$$H_{hf} = 2\left(\frac{8\pi}{3}\right)\mu_B \gamma_n \hbar \mathbf{I}\cdot\mathbf{S}(\mathbf{r})\delta(\mathbf{r})$$

$$\|H_Z\| >> \|H_Q\| >> \|H_d\|, \|H_{orb}\|$$

Fermi-Dirac

$$\frac{1}{T_1} \propto (m_e^*)^2 n_e^{\frac{2}{3}} kT$$

Maxwell-Boltzmann

$$\frac{1}{T_1} \propto (m_e^*)^{\frac{3}{2}} n_e (kT)^{\frac{1}{2}}$$

$$K = \zeta\left(\frac{8\pi}{3}\right)\gamma_e^2 h^2 \langle |u_{k(0)}|^2 \rangle_{E_0} \left(\frac{n_e}{kT}\right)$$

Dirac electrons: the case of graphene

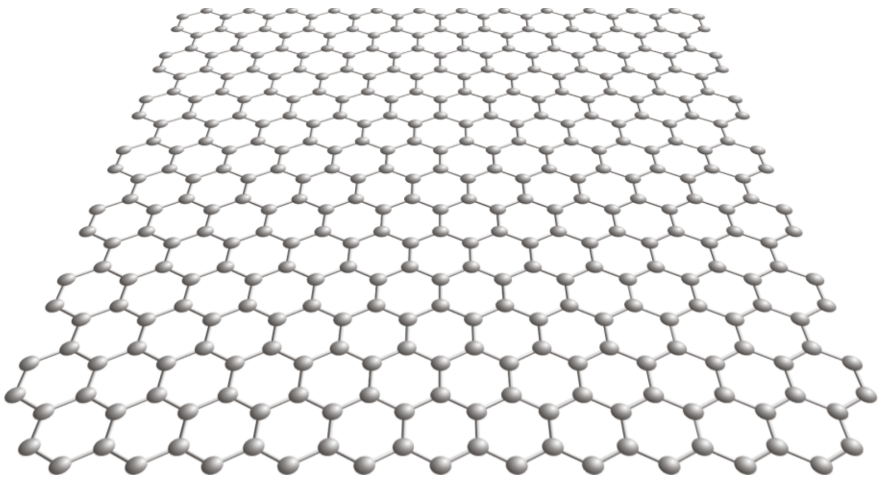

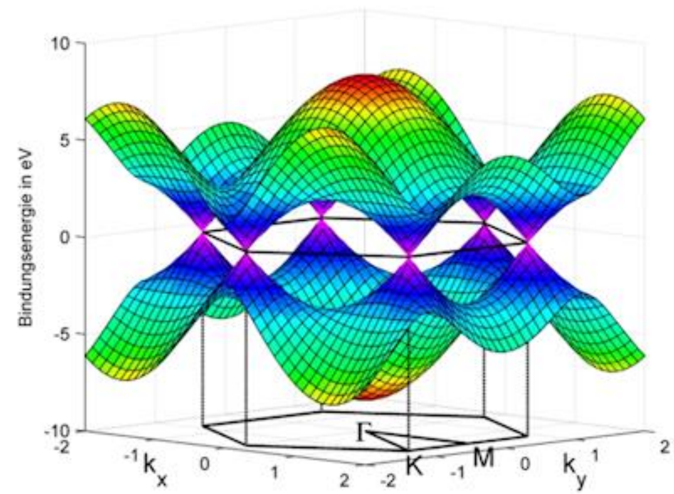

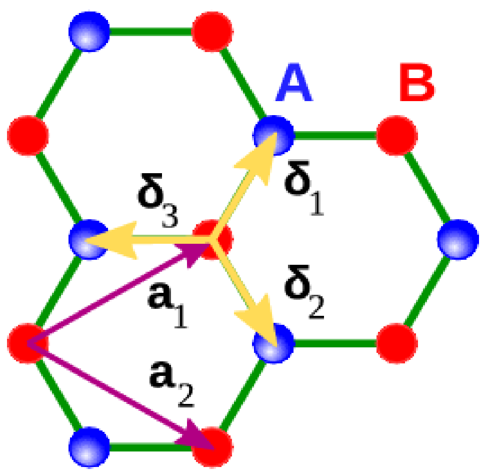

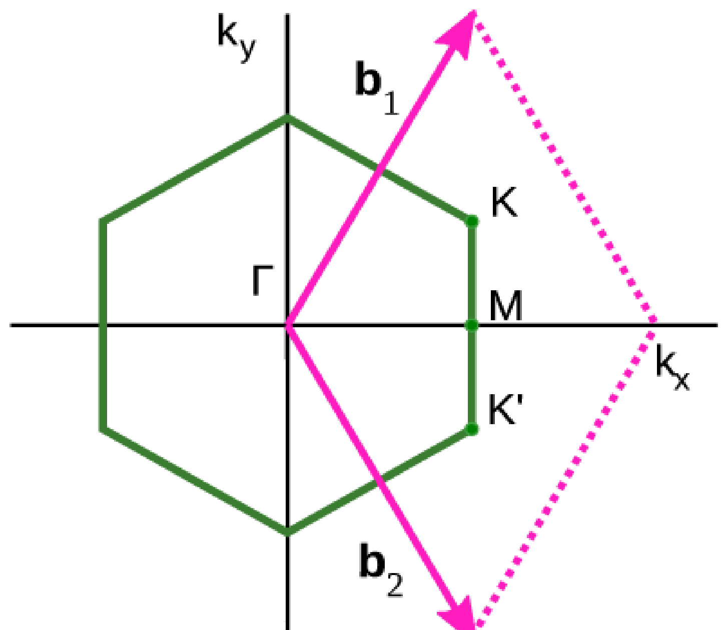

HFI (Graphene)

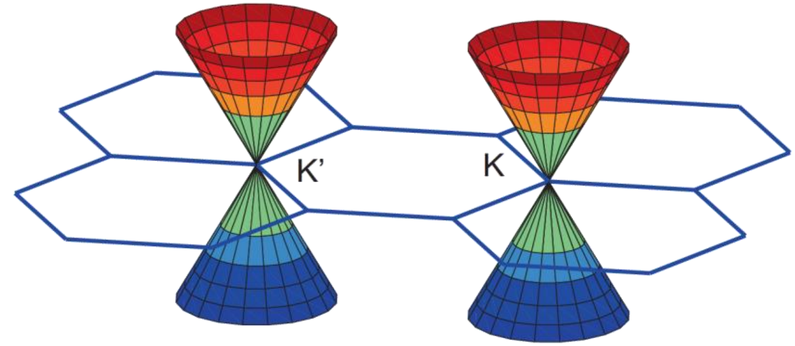

$$\boldsymbol{A}(\boldsymbol{r}) = \frac{\mu_0}{4\pi}\frac{\boldsymbol{m}\times\boldsymbol{r}}{r^3} \qquad \boldsymbol{m} = \hbar\gamma_{\rm n}\boldsymbol{I}$$

$$\boldsymbol{p} \rightarrow \boldsymbol{p} + e\boldsymbol{A}$$

$$H = \upsilon_{\rm F}\left(\sigma_x p_x + \sigma_y p_y\right) \qquad E_\alpha(\boldsymbol{k}) = \alpha\hbar v_{\rm F}|k|$$

$$\phi_{\alpha k}(\boldsymbol{r}) = \frac{1}{\sqrt{2NA_{\rm c}}}\exp(i\boldsymbol{kr})\begin{bmatrix}\alpha \\ \exp(i\varphi_k)\end{bmatrix}$$

$$A_x = -\frac{\mu_0}{4\pi}m_z y/r^3 \qquad A_y = \frac{\mu_0}{4\pi}m_z x/r^3$$

$$H_{\rm HFI,graphene} = \frac{\mu_0}{4\pi}\hbar\gamma_{\rm n}I_z\left(\frac{\boldsymbol{r}\times\boldsymbol{j}}{r^3}\right)_z \qquad \boldsymbol{j} = ev_{\rm F}\boldsymbol{\sigma}$$

$$+\frac{\mu_0}{4\pi}g\mu_{\rm B}\hbar\gamma_{\rm n}\boldsymbol{I}\left(\frac{\boldsymbol{S}r^2 - 3\boldsymbol{r}(\boldsymbol{S}\boldsymbol{r})}{r^5} - \frac{8\pi}{3}\boldsymbol{S}\delta(\boldsymbol{r})\right)$$

The orbital magnetization

$$(\boldsymbol{r} \times \boldsymbol{j})$$

(nucleus interacts with orbital motion of Dirac electron)

replaces the angular momentum operator

$$(\boldsymbol{r} \times \boldsymbol{p})$$

Electric current operator in graphene

$$\boldsymbol{j} = e v_{\mathrm{F}} \boldsymbol{\sigma}$$

If we replace j by its operator for a normal metal

$$\boldsymbol{j} = e\boldsymbol{p}/m^*$$

We formally recover the Abragam expression for HFI

$$H_{\mathrm{HFI}} = \frac{\mu_0}{4\pi} g\hbar\gamma_{\mathrm{n}} \boldsymbol{I} \Big[\mu_{\mathrm{B}}^* \frac{\boldsymbol{r} \times \boldsymbol{p}}{\hbar r^3} + \mu_{\mathrm{B}} \Big(\frac{\boldsymbol{S} r^2 - 3r(\boldsymbol{S} r)}{r^5} - \frac{8\pi}{3} \boldsymbol{S} \delta(\boldsymbol{r}) \Big) \Big]$$

v_F~5×10^5 m/s or ~0.7 eV vs 10^{-6} eV for usual HFI

HFI (TI surface state)

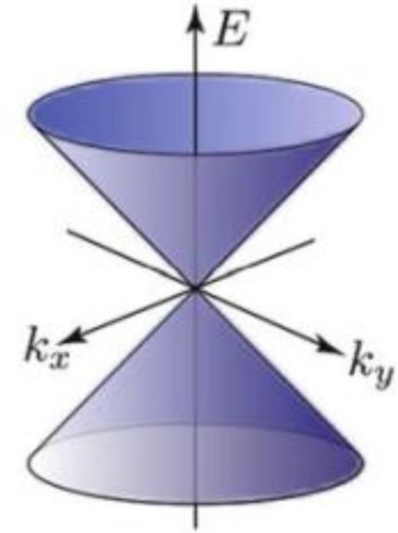

y-z plane at $x = 0$

$$\Delta H_{3D} = vp_y\alpha_y + vp_z\alpha_z - B(p_y^2 + p_z^2)\beta$$

$$\begin{aligned} H_{eff} &= \frac{1}{2}(\langle\Phi_1|, \langle\Phi_2|)\Delta H_{3D}\begin{pmatrix} |\Phi_1\rangle \\ |\Phi_2\rangle \end{pmatrix} \\ &= v\mathrm{sgn}(B)(p_y\sigma_y + p_z\sigma_z). \end{aligned}$$

$$E_p = \pm vp$$

$$\Psi_\pm = C\Psi_\pm^0(e^{-x/\xi_+} - e^{-x/\xi_-})\exp[+i\,(p_y y + p_z z)\,/\hbar]$$

$$\Psi_+^0 = \begin{pmatrix} \cos\frac{\theta}{2}\mathrm{sgn}(B) \\ -i\sin\frac{\theta}{2}\mathrm{sgn}(B) \\ \sin\frac{\theta}{2} \\ i\cos\frac{\theta}{2} \end{pmatrix} \quad \Psi_-^0 = \begin{pmatrix} \sin\frac{\theta}{2}\mathrm{sgn}(B) \\ i\cos\frac{\theta}{2}\mathrm{sgn}(B) \\ -\cos\frac{\theta}{2} \\ i\sin\frac{\theta}{2} \end{pmatrix}$$

$$\xi_\pm^{-1} = \frac{v}{2\,|B|\,\hbar}\left(1 \pm \sqrt{1 - 4mB + 4B^2p^2/\hbar^2}\right) \qquad p = \sqrt{p_y^2 + p_z^2}$$

Topological Insulators

Studies of Surface States SSNMR

Studies of Bulk Properties

Topological Crystalline Insulators

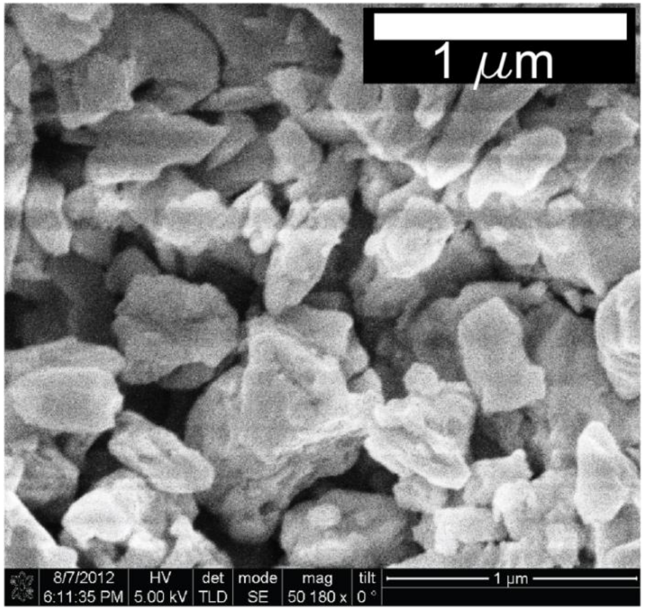

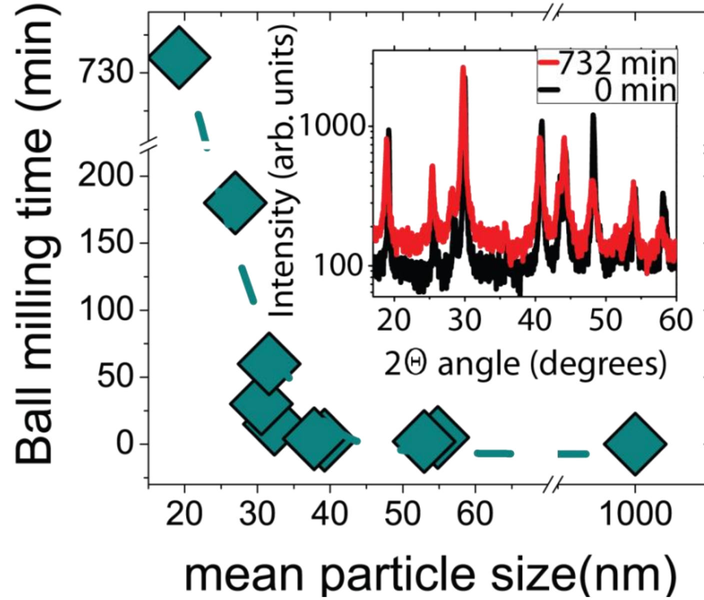

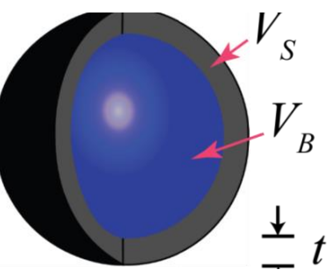

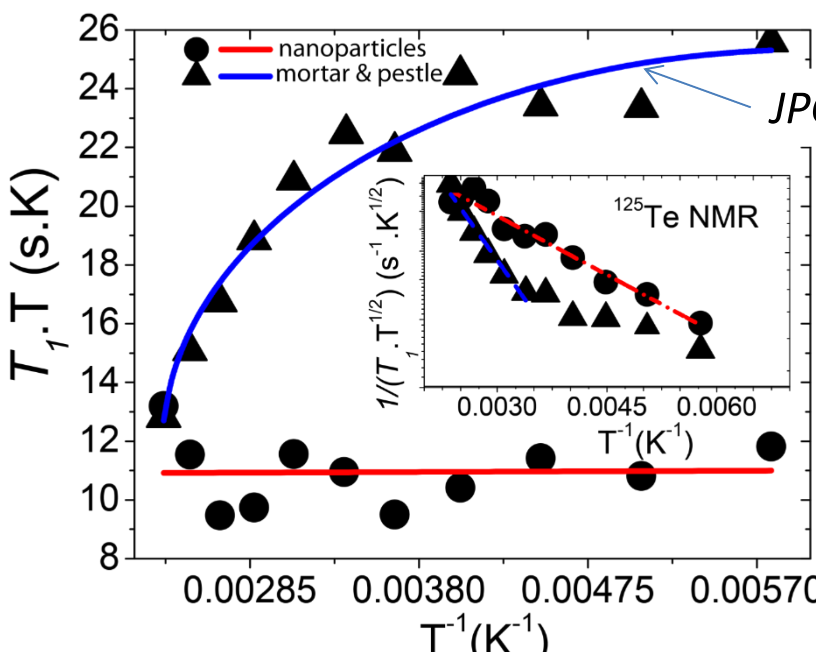

JPCC **116**, 17300 (2012)

Koumoulis D, et al., Phys. Rev. Lett. **110**, 026602 (2013)

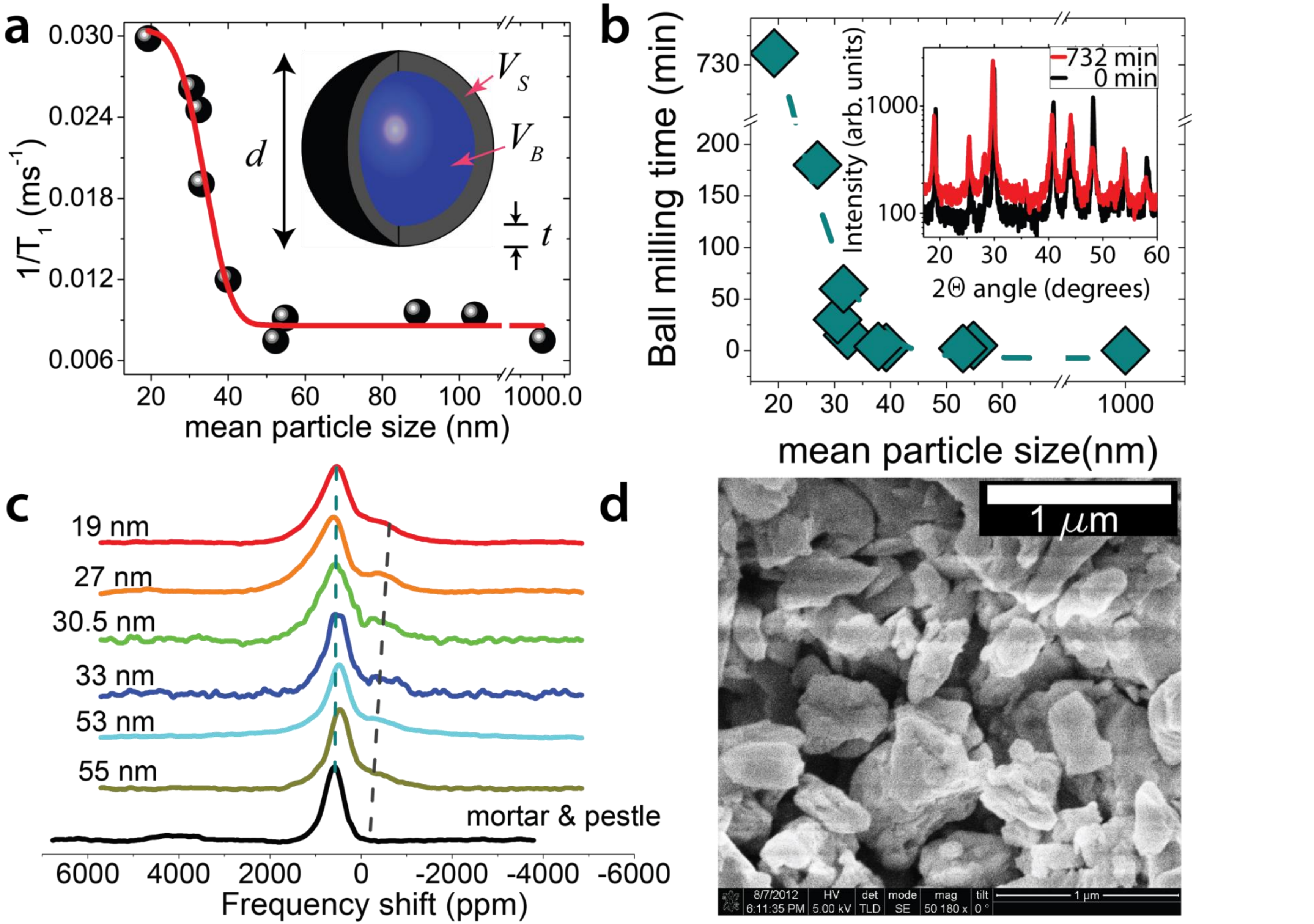

Koumoulis D, Phys. Rev. Lett. **110**, 026602 (2013)

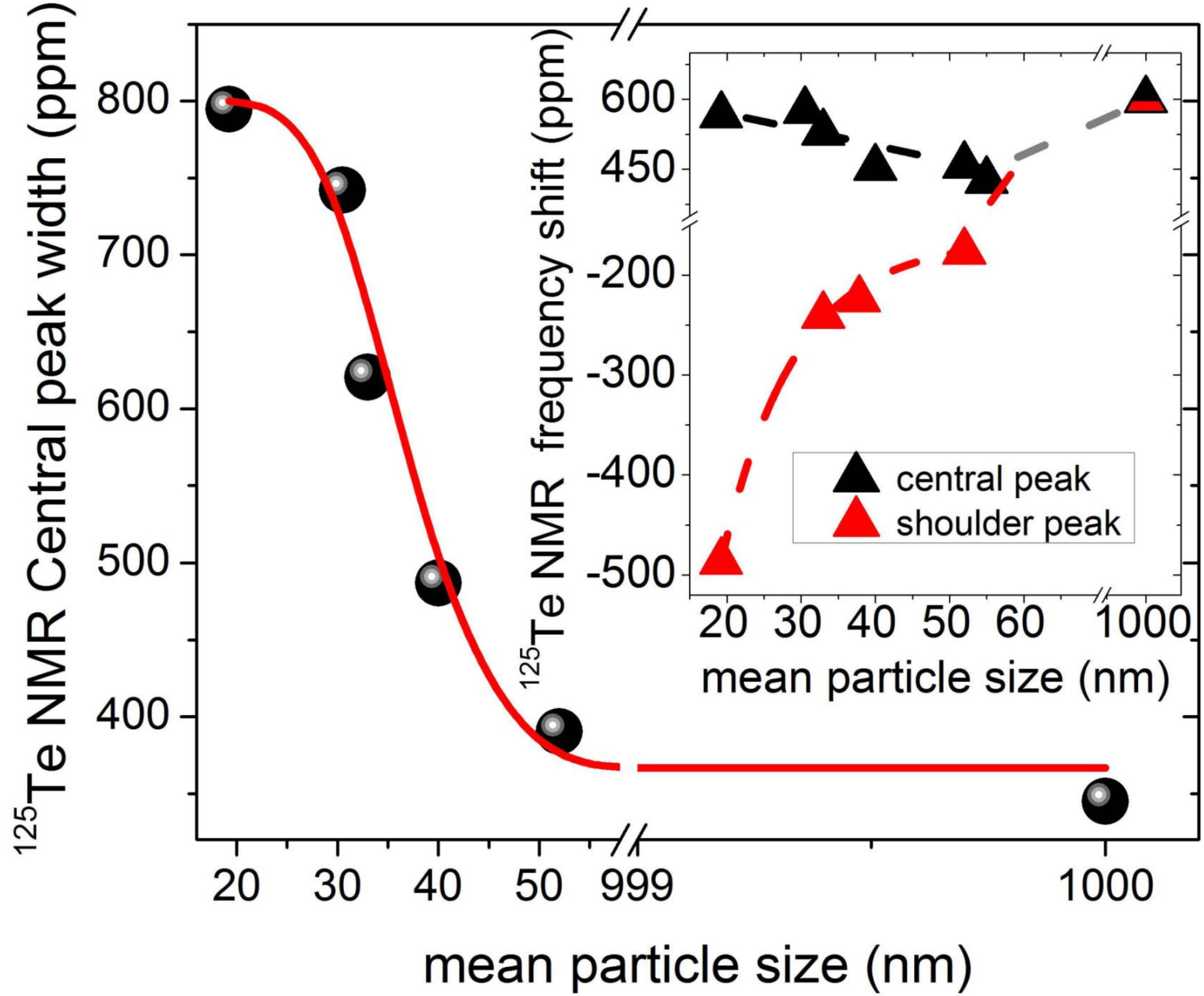

Koumoulis D, Phys. Rev. Lett. **110**, 026602 (2013)

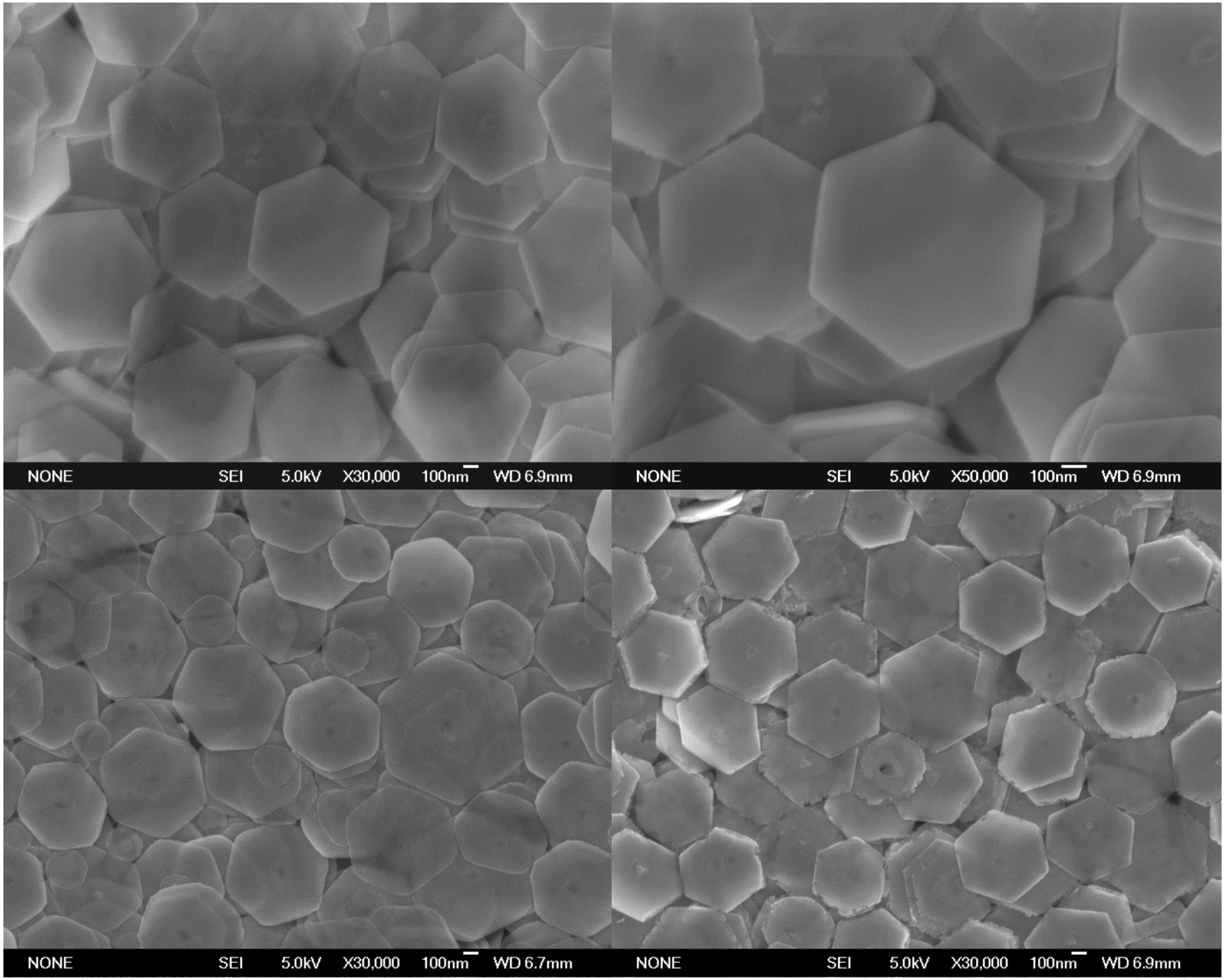
NONE SEI 5.0kV X30,000 100nm WD 6.9mm
NONE SEI 5.0kV X50,000 100nm WD 6.9mm
NONE SEI 5.0kV X30,000 100nm WD 6.7mm
NONE SEI 5.0kV X30,000 100nm WD 6.9mm

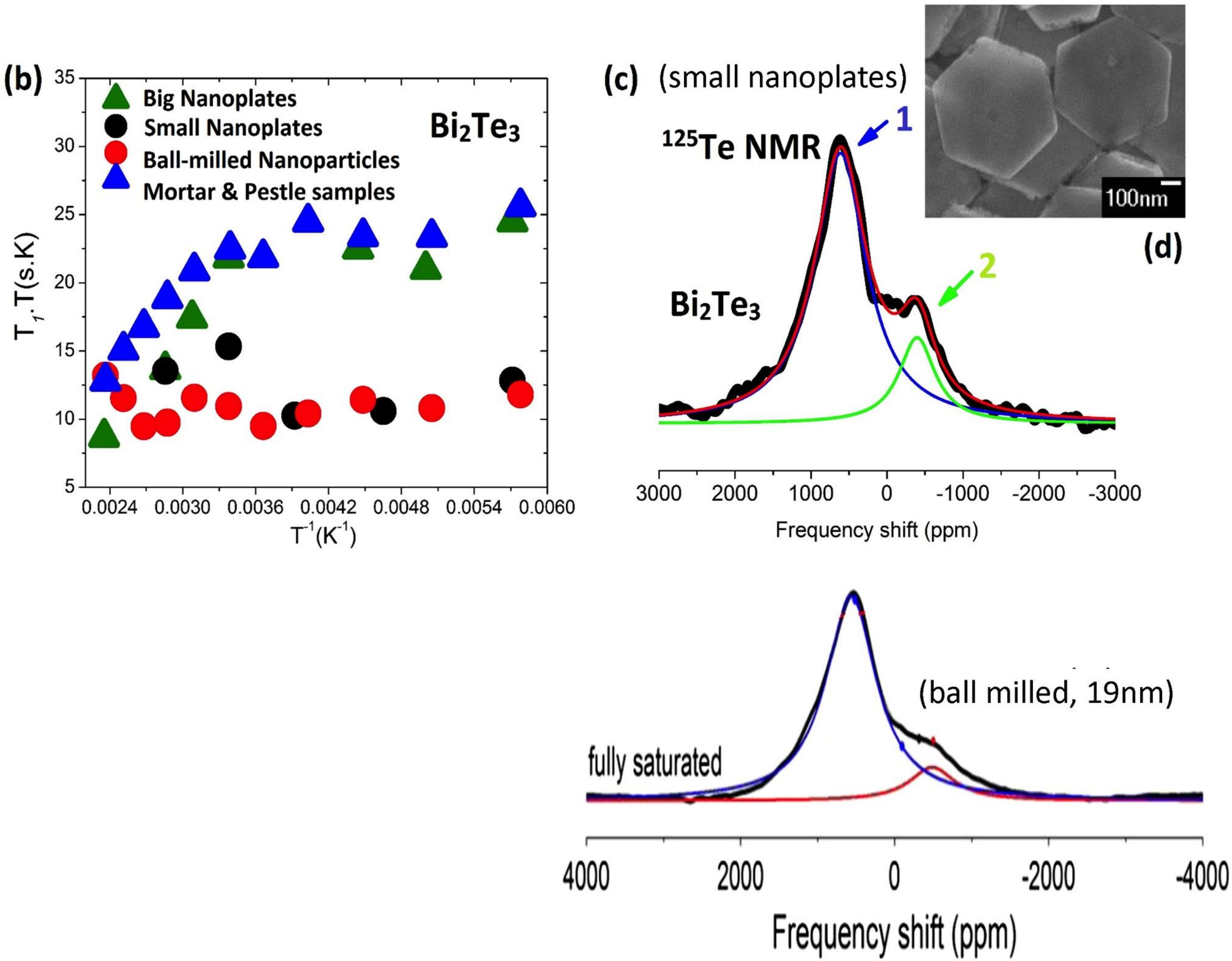

(b)
Big Nanoplates
Small Nanoplates
Ball-milled Nanoparticles
Mortar & Pestle samples
Bi_2Te_3
$T_1.T(s.K)$
$T^{-1}(K^{-1})$
0.0024
0.0030
0.0036
0.0042
0.0048
0.0054
0.0060
5
10
15
20
25
30
35
(c) (small nanoplates)
^{125}Te NMR
1
2
Bi_2Te_3
3000
2000
1000
0
-1000
-2000
-3000
Frequency shift (ppm)
100nm
(d)
(ball milled, 19nm)
fully saturated
4000
2000
0
-2000
-4000
Frequency shift (ppm)

Topological Insulators

Studies of Surface States Quadrupolar NMR

Studies of Bulk Properties

Topological Crystalline Insulators

^{121}Sb nuclei (I=5/2)

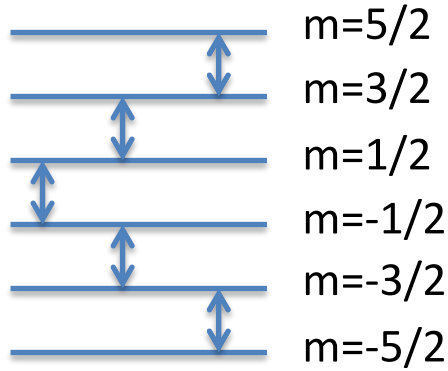

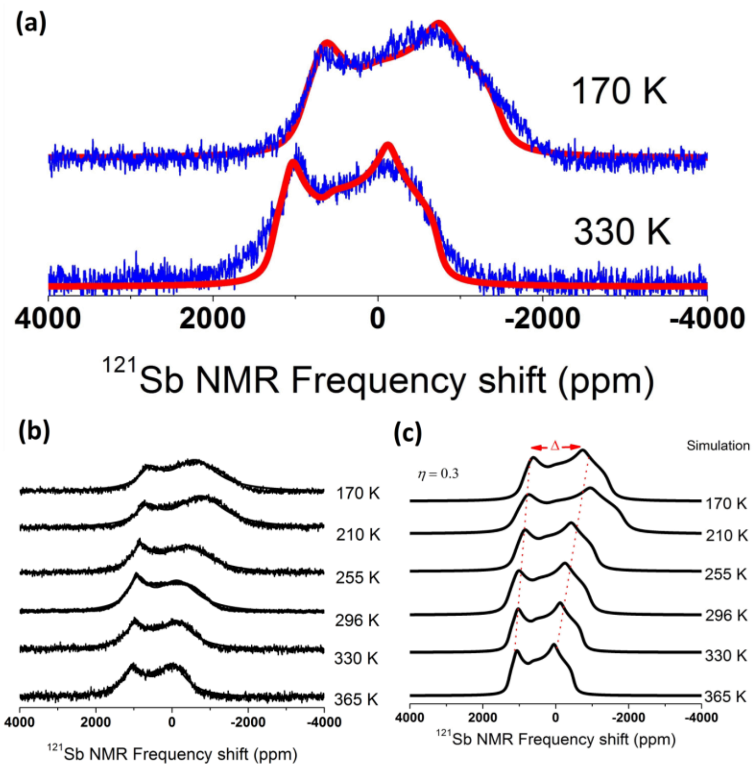

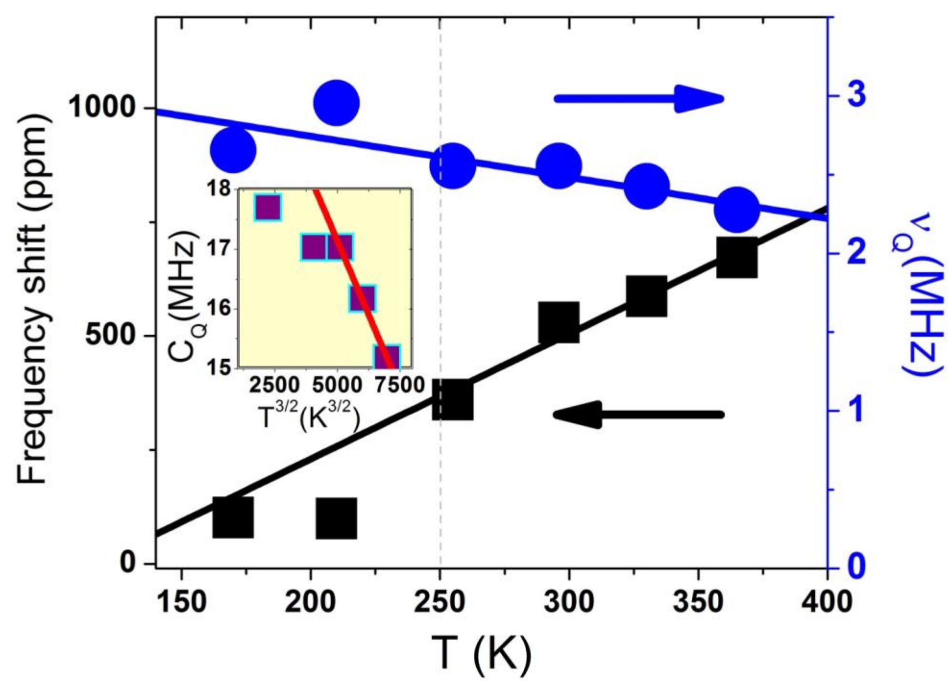

^{121}Sb vs T for Sb_2Te_3

^{121}Sb nuclei (I=5/2)

$$\frac{M(t)}{M(0)} = 1 - \frac{2}{35}\exp\left(-\left[\frac{t}{T_1}\right]^b\right) - \frac{16}{45}\exp\left(-\left[\frac{6t}{T_1}\right]^b\right) - \frac{100}{63}\exp\left(-\left[\frac{15t}{T_1}\right]^b\right)$$

^{123}Sb nuclei (I=7/2)

$$\frac{M(t)}{M(0)} = 1 - \frac{1}{84}\exp\left(-\left[\frac{t}{T_1}\right]^b\right) - \frac{3}{44}\exp\left(-\left[\frac{6t}{T_1}\right]^b\right) - \frac{75}{364}\exp\left(-\left[\frac{15t}{T_1}\right]^b\right) - \frac{1225}{1716}\exp\left(-\left[\frac{28t}{T_1}\right]^b\right)$$

magnetic relaxation mechanism

$$\frac{121_{(\frac{1}{T_1})}}{123_{(\frac{1}{T_1})}} = \frac{121_{\gamma_n^2}}{123_{\gamma_n^2}} = 3.41$$

electric relaxation mechanism

$$\frac{121_{(\frac{1}{T_1})}}{123_{(\frac{1}{T_1})}} = \frac{(121_Q)^2 \times \frac{(2I+3)}{I^2(2I+1)}}{(123_Q)^2 \times \frac{(2I+3)}{I^2(2I+1)}} = 1.44$$

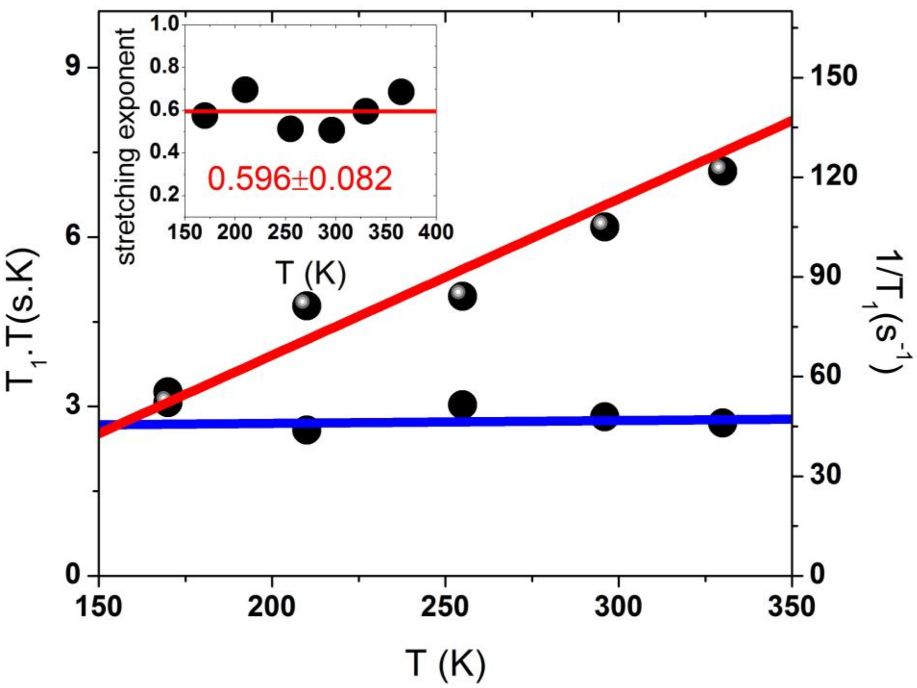

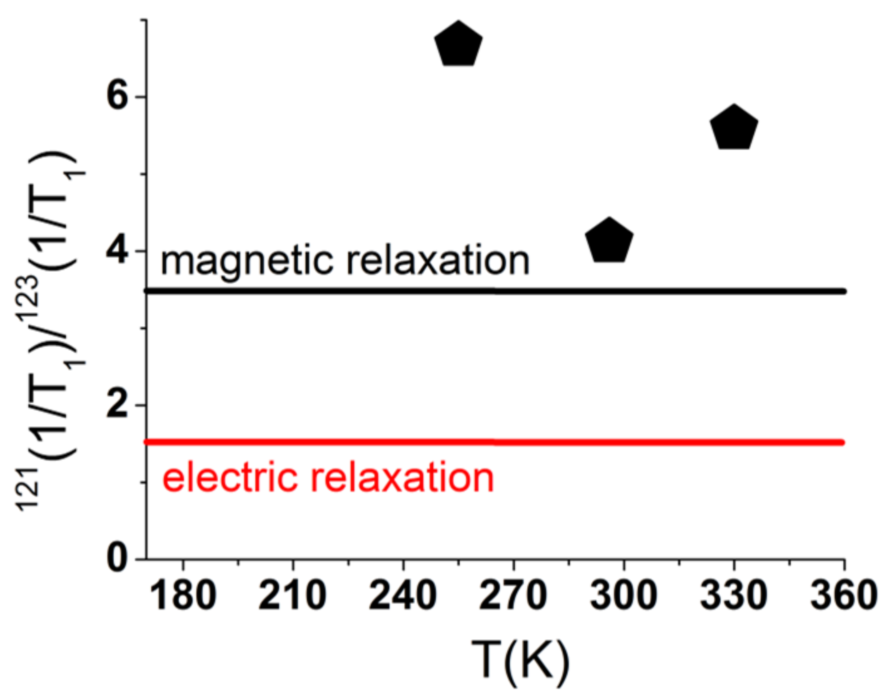

Topological Insulators

Studies of Surface States βNMR

Studies of Bulk Properties

Topological Crystalline Insulators

ion beam techniques @ TRIUMF

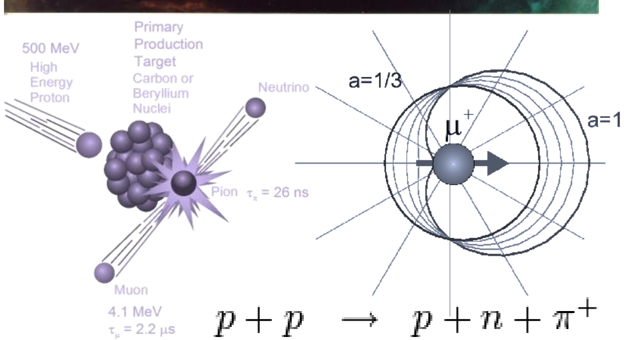

$$p + p \rightarrow p + n + \pi^+$$
$$p + n \rightarrow n + n + \pi^+$$

M1351 – Study of Vacancy Detects in TIs
M1352 – Studies of Interface Phenomena involving TIs
M1399 – betaNMR studies of topological crystalline insulator states
M1438 – βNMR investigations of the topological magneto-electric effect

NMR vs Nuclear Detected Methods

	NMR	μSR	β-NMR
Polarization	<0.01	>0.8	
detection method	electronic pickup	anisotropic β decay	
Sensitivity	10^{17} spins	10^{7} spins	
T_1 range (s)	$10^{-5} - 10^{2}$	$10^{-8} - 10^{-4}$	$10^{-3} - 10^{3}$
range	N/A		
0.5 mm	10 Å –3000 Å*		
Applied field	high	any	small-high

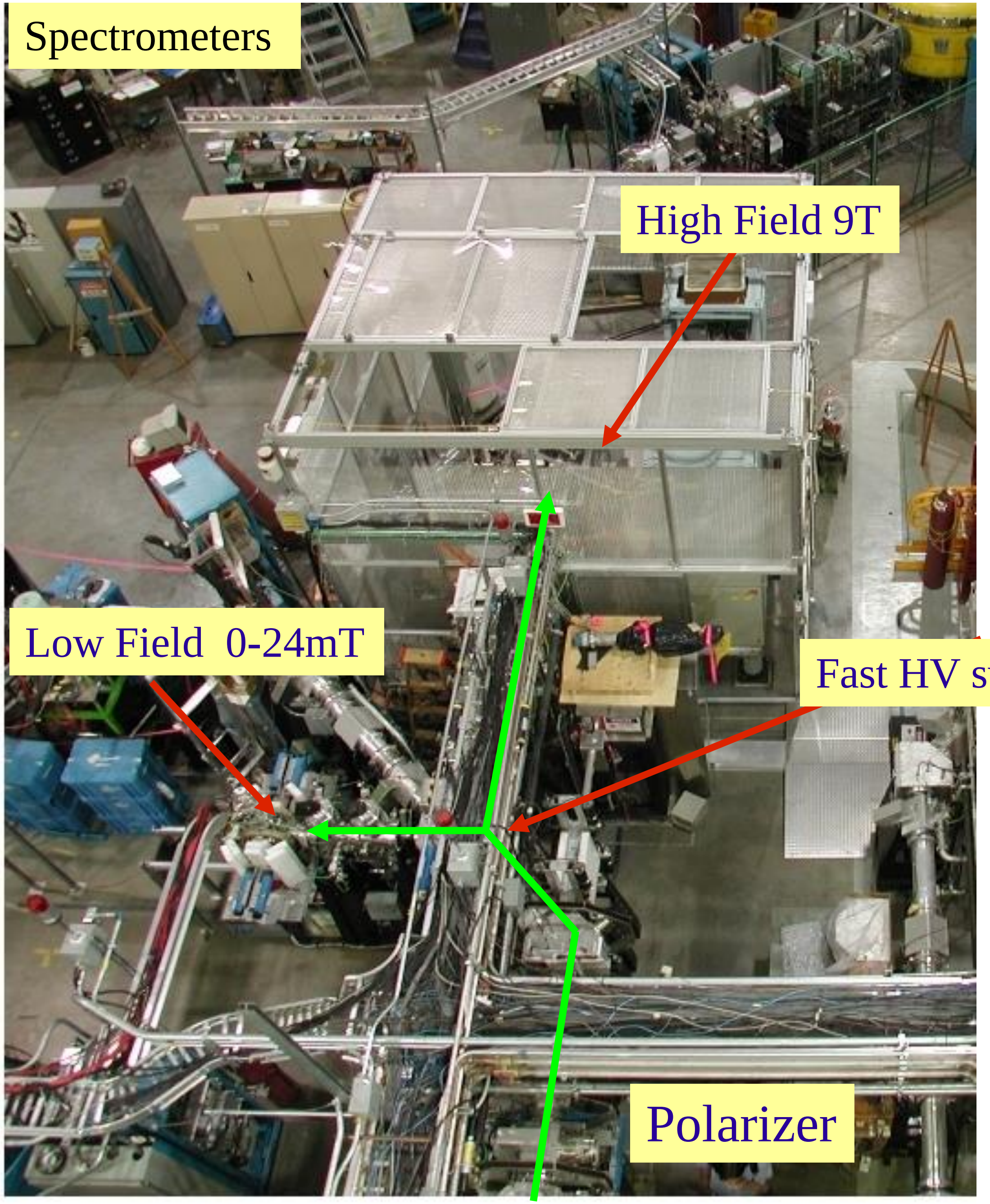

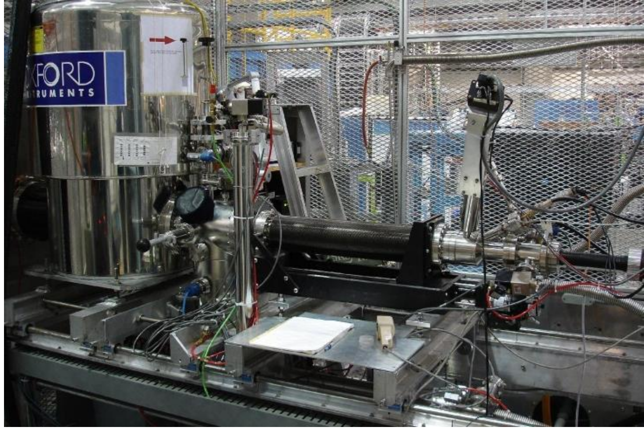

High Field Spectrometer:

H_0 : 0.1 – 9 T

E_{Li} : 0.1 – 30 keV

T : 3 – 300 K

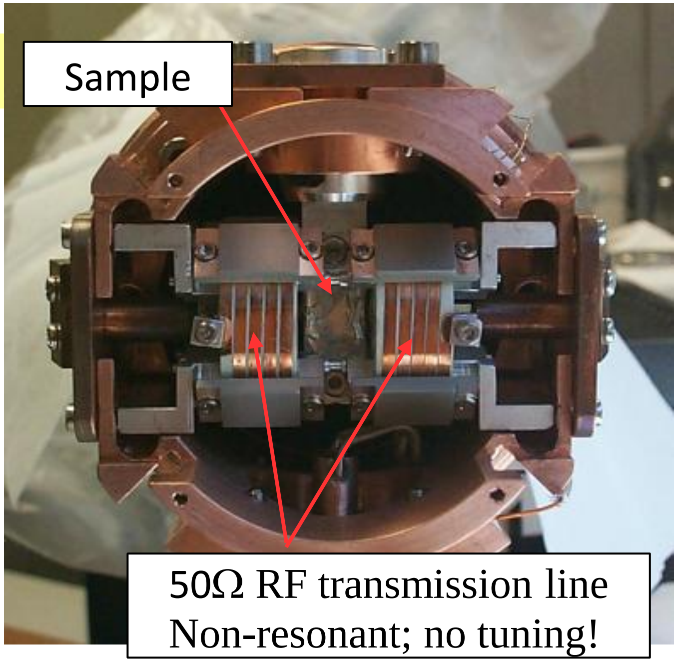

M1352: TI/OI thin-film heterostructure

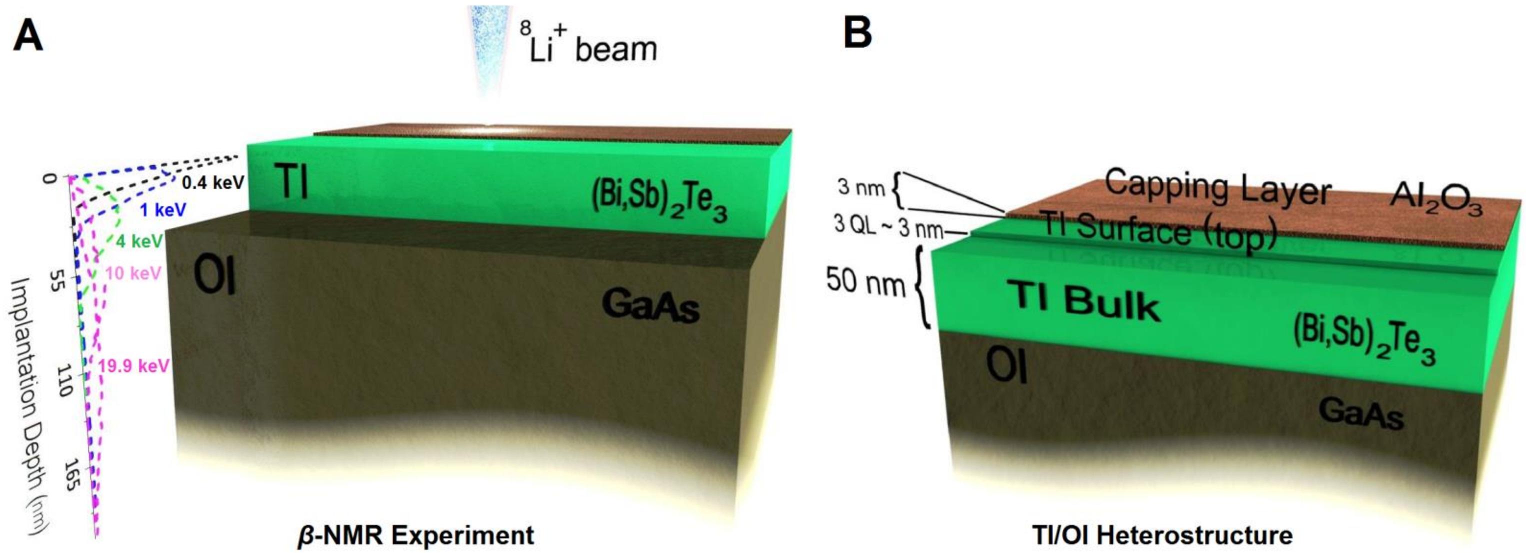

0.4 keV, 50% signal originates from TI surface, d=4 ± 3 nm
1 keV , 80% originates from TI bulk

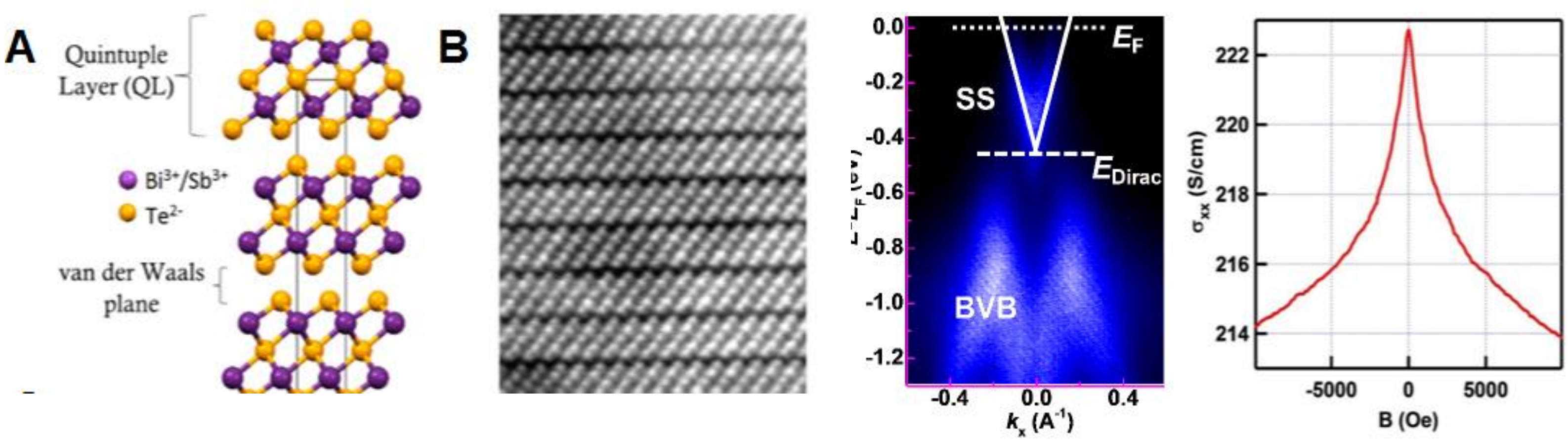

Knight shift measures carrier concentration, s-o mixing, density of states @E_F

$$K = \frac{4\pi}{3} g . g^{*} . \mu_B^2 . \langle |u_k(0)|^2 \rangle_{E_0} \rho(E_F)$$

$$(\cos^2\theta^+)\langle R|\Delta(\vec{r})|R\rangle$$

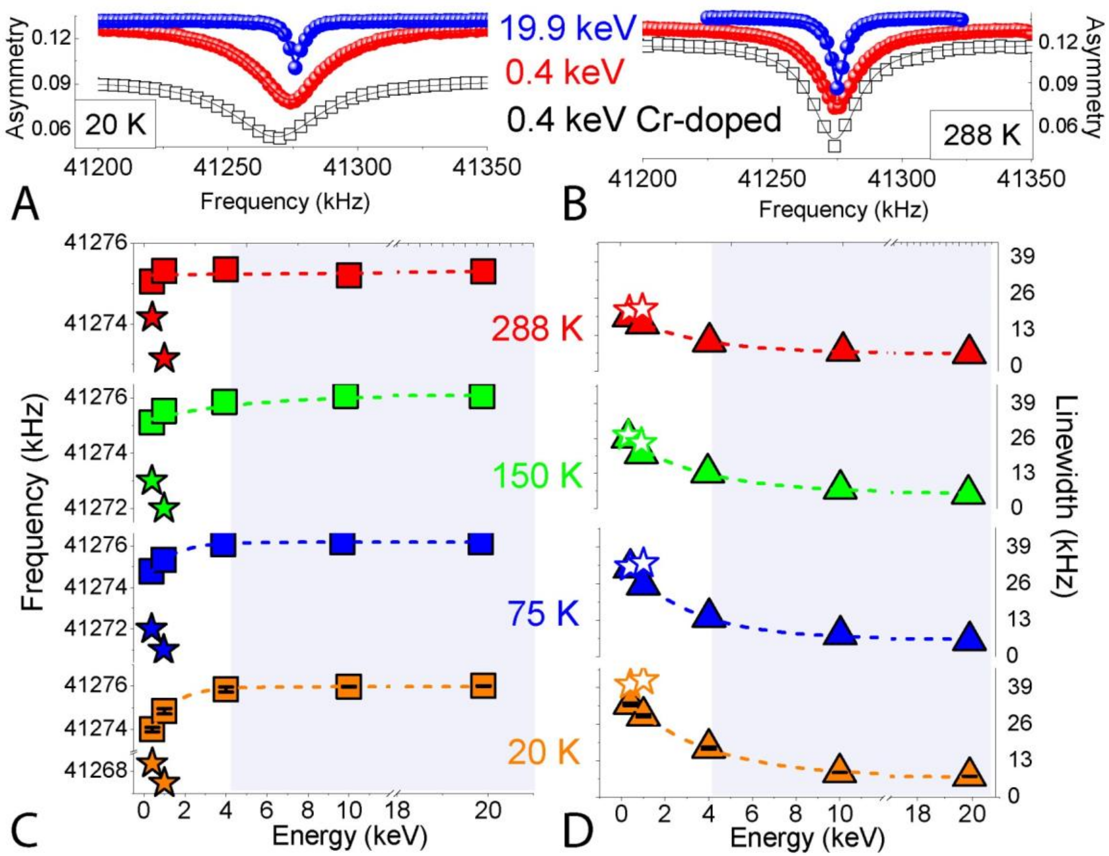

M1352: Knight Shift, hyperfine constant, local carrier concentration

$$K = \frac{\nu - \nu_{ref}}{\nu_{ref}} \qquad K_d = K + \left(\frac{8\pi}{3}\right)\cdot\chi \qquad A_{hf} = \frac{K \cdot N_A \cdot \mu_e}{n \cdot \chi}$$

$$K = \zeta \frac{8\pi}{3} \gamma_e^2 h^2 \langle |u_k(0)|^2 \rangle_{E_0} \frac{n_e}{kT}$$

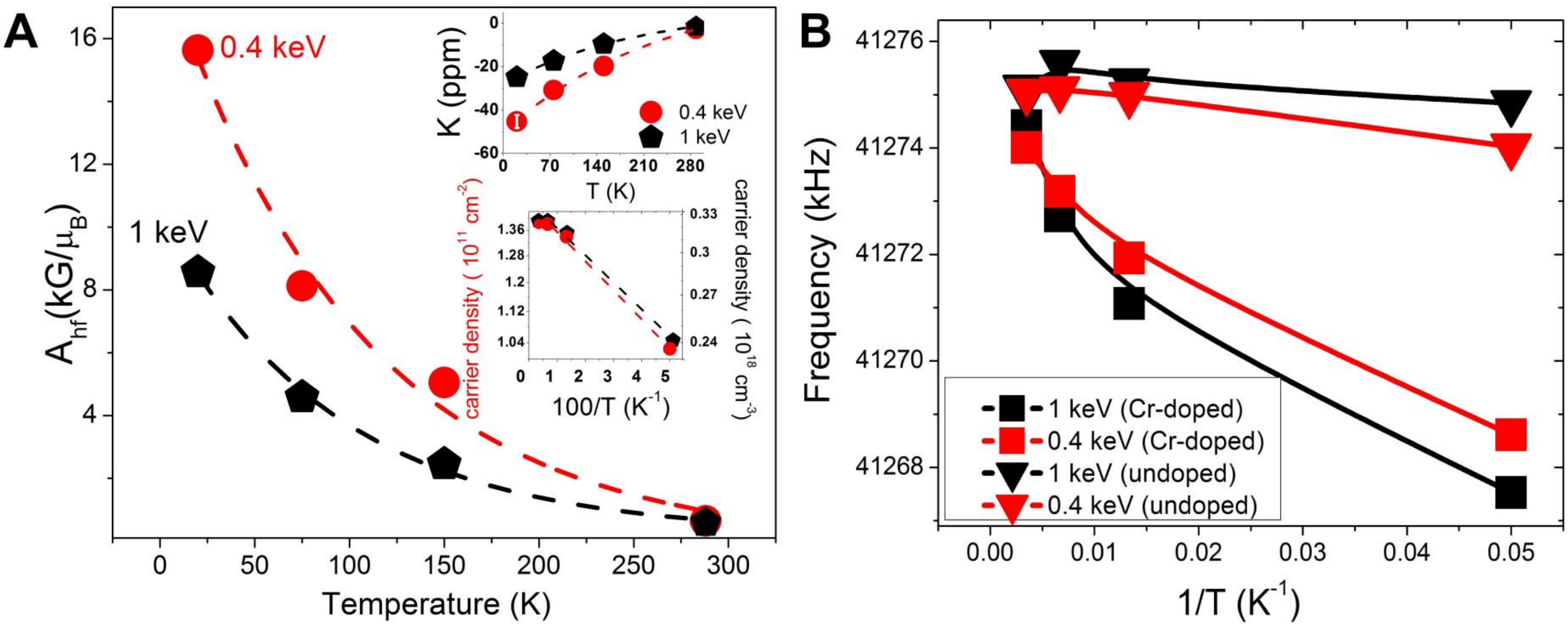

D. Koumoulis et al. (submitted)

depth-resolved magnetic properties

$$\Delta w = \frac{W_{CrTI} - W_{TI}}{W_{TI}}$$

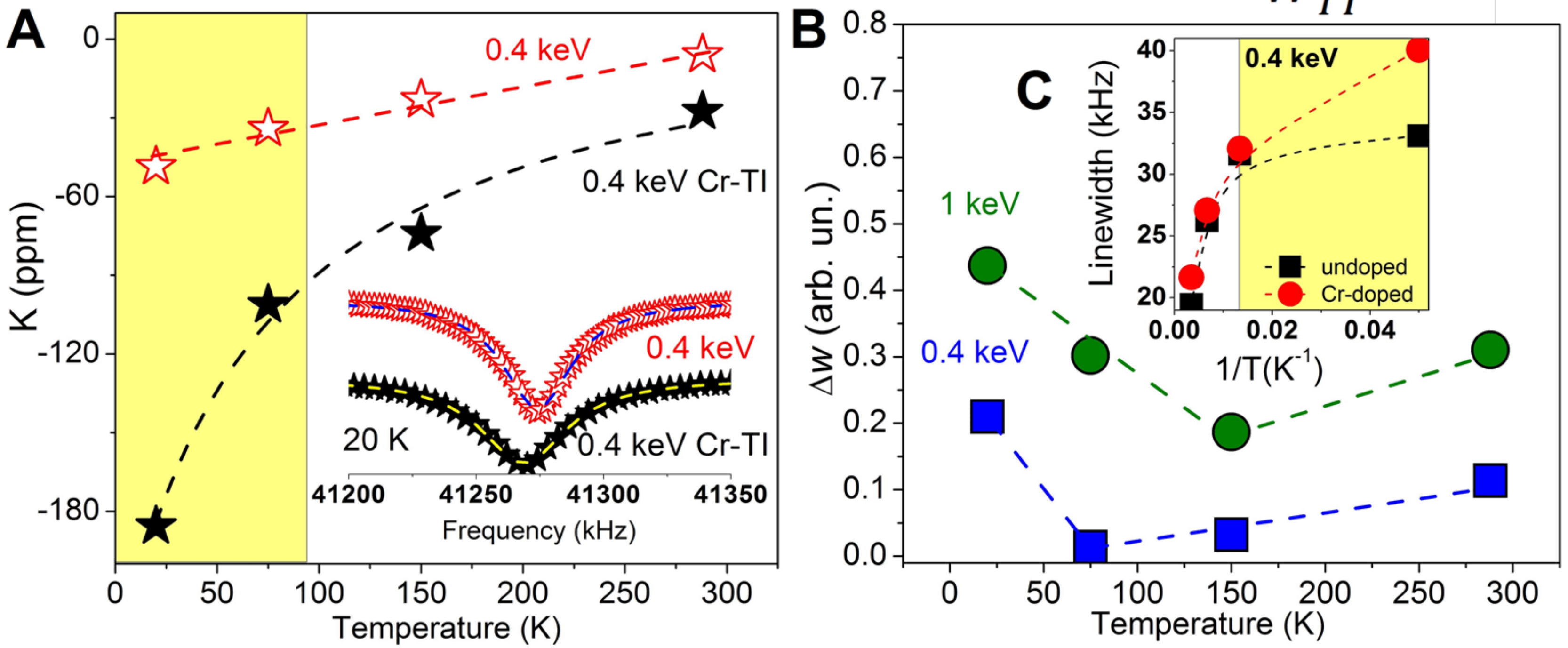

$$\frac{W_{CrTI} - W_{TI}}{W_{TI}} = \left(\frac{Jp^2C}{3gk_B}\right) \cdot \frac{1}{T} + D$$

$$J^{surface} = 0.9 \cdot J^{bulk}$$

p effective number of Bohr magnetons

C atomic fraction of paramagnetic atoms

D temperature independent term

g electron *g*-factor

J effective *s*-*d* exchange integral

negative Knight shift observed in $BiSbTe_3$ nanoparticles

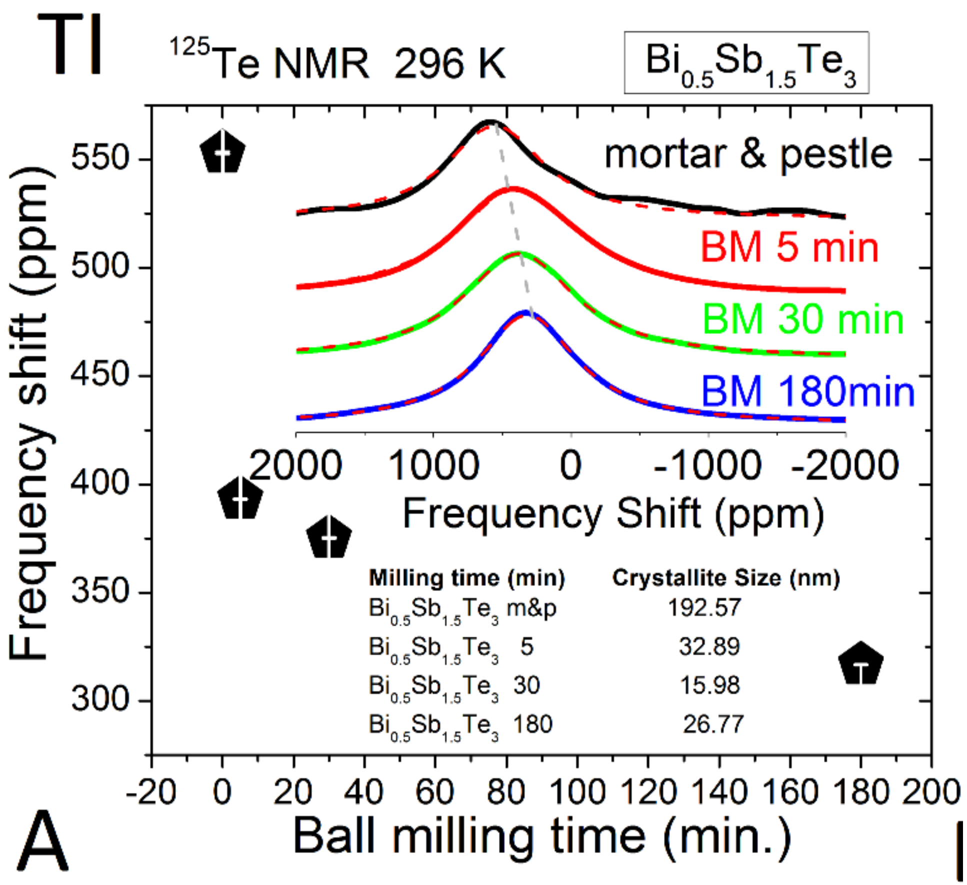

trivial insulators do not show depth or particle size dependence

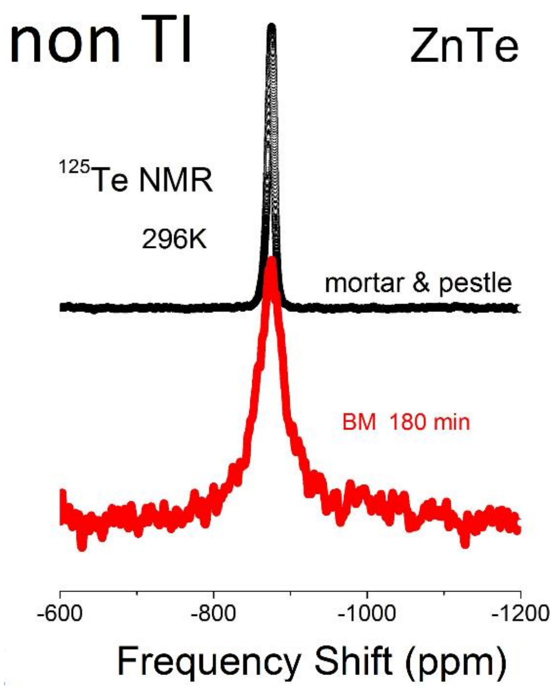

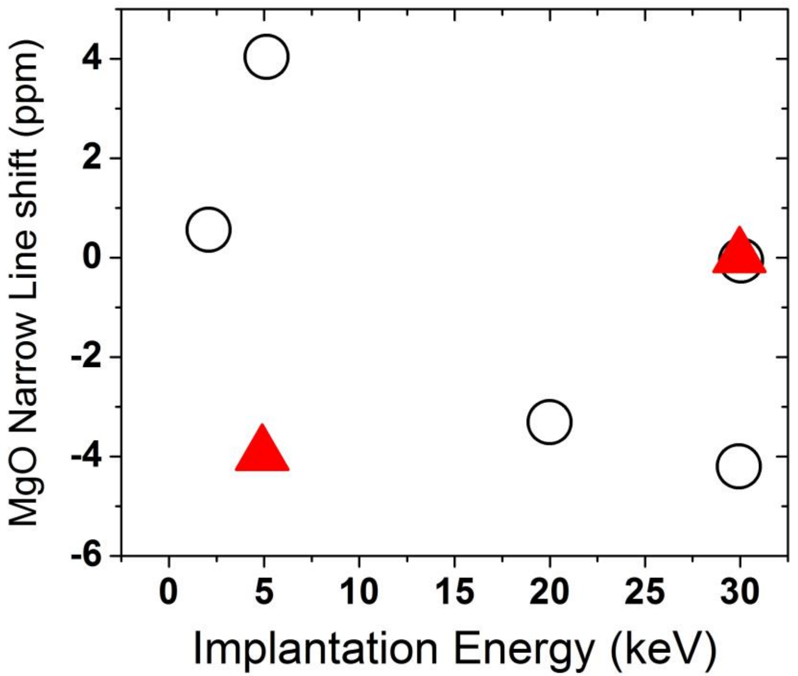

Topological Insulators

Studies of Surface States

Studies of Bulk Properties

Topological Crystalline Insulators

topological crystalline insulator has even number of Dirac cones

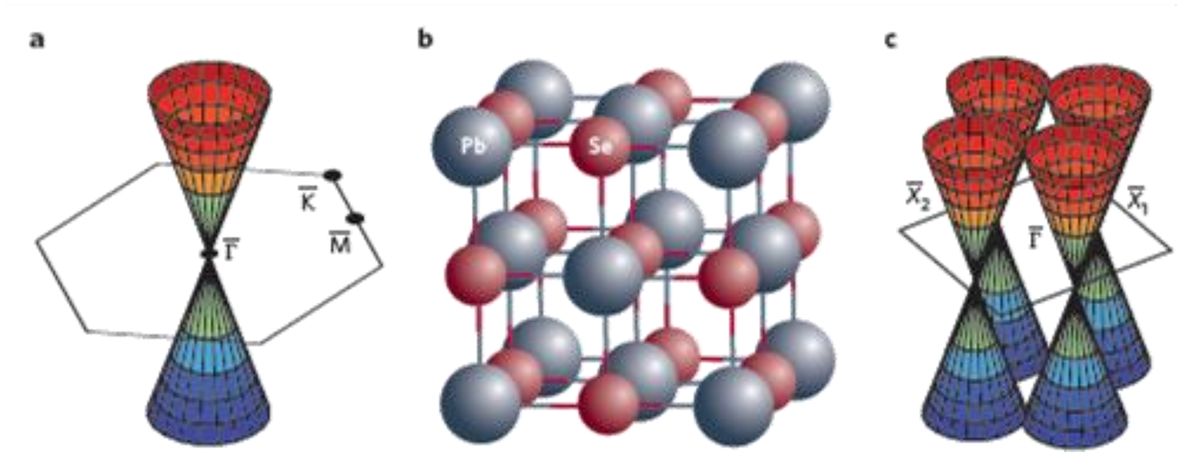

$Pb_{1-x}Sn_xSe$

Crystalline symmetry replaces time-reversal symmetry

Surface states protected by crystal mirror symmetry

Only on crystal faces perpendicular to the mirror planes

Fu, L. *Phys. Rev. Lett.* **106**, 106802 (2011); Hsieh, T. H. et al. *Nature Comm.* **3**, 982 (2012).

β-NMR , ARPES and Transport

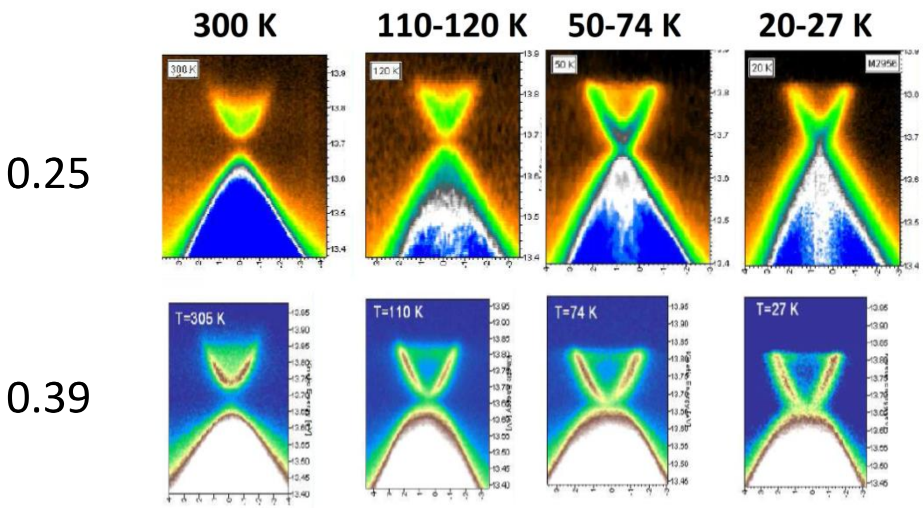

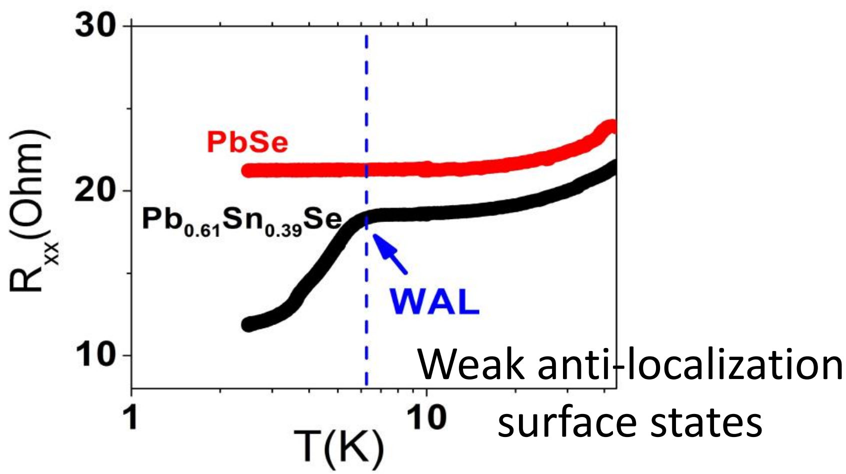

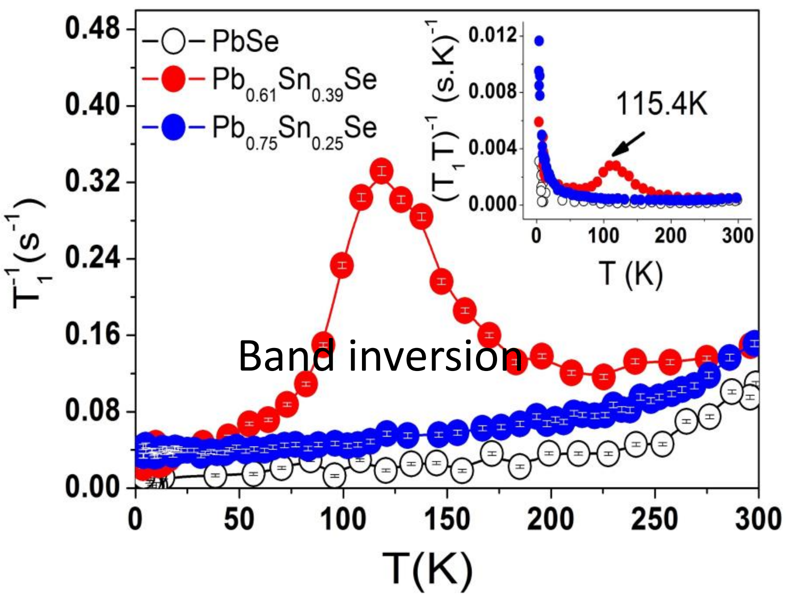

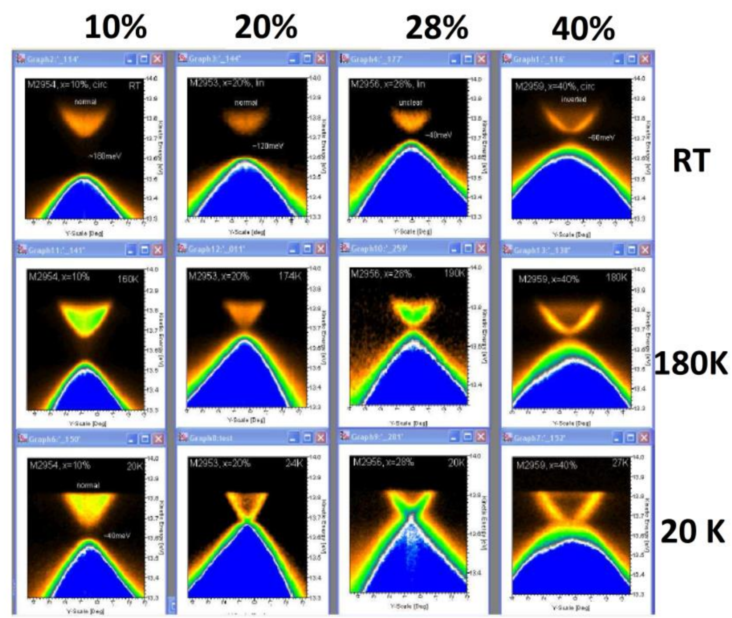

2 keV beam energy, $Pb_{0.61}Sn_{0.39}Se$ (red), $Pb_{0.75}Sn_{0.25}Se$ (blue), and PbSe (white) , H_o = 6.55 T

in summary, nuclear spin dipole and quadrupole moments provide signatures for

topological surface states in TIs

bulk properties, including defects

topological crystalline insulators

new techniques could be useful for:
use near room temperature, p-type materials,
studies of materials with high defect content

acknowledgments

Dimitrios Koumoulis

Robert Taylor

Kang L Wang

Liang He

Xufeng Kou

Zhenxing Wang

Gerald Morris (TRIUMF)

Greg A. Fiete (UT Austin)

Mercouri Kanatzidis (NWU)

Thomas Chasapis (NWU)

G. Springholz (Linz)

MTO DARPA

MICROSYSTEMS TECHNOLOGY OFFICE